Geophysical Research Letters

RESEARCH LETTER
10.1029/2018GL078697

Key Points:
- Occator crater hosts ring-mold craters that are morphologically similar to those on Mars
- Ring-mold craters on Ceres are likely formed by impacts into ice covered by a thin layer of regolith
- The formation of ring-mold craters is a sign of water ice reservoirs in the subsurface

Correspondence to:
K. Krohn,
katrin.krohn@dlr.de

Citation:
Krohn, K., Neesemann, A., Jaumann, R., Otto, K. A., Stephan, K., Wagner, R. J., et al. (2018). Ring-mold craters on Ceres: Evidence for shallow subsurface water ice sources. *Geophysical Research Letters*, *45*, 8121–8128. https://doi.org/10.1029/2018GL078697

Received 15 MAY 2018
Accepted 10 AUG 2018
Accepted article online 20 AUG 2018
Published online 28 AUG 2018

Ring-Mold Craters on Ceres: Evidence for Shallow Subsurface Water Ice Sources

K. Krohn[1], A. Neesemann[2], R. Jaumann[1,2], K. A. Otto[1], K. Stephan[1], R. J. Wagner[1], F. Tosi[3], F. Zambon[3], O. Ruesch[4], D. A. Williams[5], C. A. Raymond[6], and C. T. Russell[7]

[1]Institute of Planetary Research, German Aerospace Center (DLR), Berlin, Germany, [2]Institute of Geological Sciences, Planetary Sciences and Remote Sensing, Freie Universität Berlin, Berlin, Germany, [3]INAF-IAPS, National Institute for Astrophysics, Rome, Italy, [4]ESTEC, European Space Agency, Noordwijk, The Netherlands, [5]School of Earth and Space Exploration, Arizona State University, Tempe, AZ, USA, [6]NASA JPL, California Institute of Technology, Pasadena, CA, USA, [7]UCLA, Los Angeles, CA, USA

Abstract One of the main tasks of the Dawn mission is to characterize the potentially ice-rich crust of the dwarf planet Ceres. Ongoing studies reveal morphological features related to ice-rich material such as pits or particular landslides. Here we report the identification of ring-mold craters within the huge impact crater Occator. The Cerean ring-mold craters exhibit strong morphological similarities to the ring-mold craters on Mars, where ice-rich material is thought to be involved in such crater development. We discuss the occurrence of water ice reservoirs in the subsurface and assume that ice-rich material likely plays an important role in the development of ring-mold craters on Ceres. The occurrence of ring-mold craters on the surface of Ceres is not only a sign of water ice reservoirs in the subsurface but can also be used for the study of habitable zones on planetary bodies.

Plain Language Summary One of the main tasks of the Dawn mission is to characterize the potentially ice-rich crust of the dwarf planet Ceres. Ongoing studies reveal morphological features related to ice-rich material such as pits or particular landslides. Here we report the identification of a special type of craters, so-called ring-mold craters. The craters are found within the huge impact crater Occator. The Cerean ring-mold craters exhibit strong morphological similarities to the ring-mold craters on Mars, where ice-rich material is thought to be involved in such crater development. We discuss the occurrence of water ice reservoirs in the subsurface and assume that ice-rich material likely plays an important role in the development of ring-mold craters on Ceres. The occurrence of ring-mold craters on the surface of Ceres is not only a sign of water ice reservoirs in the subsurface but can also be used for the study of habitable zones on planetary bodies.

1. Introduction

Since the Dawn spacecraft arrived at Ceres in March 2015, Framing Camera (FC) data (Sierks et al., 2011) have shown a diversity of crater morphologies on the dwarf planet (Buczkowski et al., 2016; Krohn et al., 2016). We have observed small craters with an unusual concentric morphology, similar to the ring-mold craters on Mars (Kress & Head, 2008). We found different shapes of ring-mold craters adjacent to small bowl-shaped craters on the floor of the Occator crater. The ring-mold craters on Ceres contain either a central pit, bowl, or a central peak.

Ring-mold craters are common on lineated and lobated debris aprons, filling valleys, and concentric crater fills on Mars (Baker et al., 2010; Kress & Head, 2008, 2009). They are interpreted as impacts into ice covered by a thin layer of regolith. Ring-mold craters have diameters between 167 and 697 m and are generally surrounded by a rimless, circular moat. Furthermore, ring-mold craters show a variety of complex interior features. Kress and Head (2008) found four morphological types of ring-mold craters: (1) a central pit or bowl; (2) a central plateau; (3) a multiring; and (4) central mound craters.

Mangold (2003) found that ring-mold craters are generally larger than bowl-shaped craters and that they have to be infilled and deflated. Thus, they are supposed to be part of a continuum of crater modification. Kress and Head (2008), however, interpreted the size of ring-mold craters, as well as the unusual morphology, to be the result of impact through a layer of regolith-like sublimation till into a subsurface glacial deposit. Small bowl-shaped craters are primarily formed on the regolith layer and do not hit the ice-rich layer.

The potential presence of water ice within Ceres's crust modeled by McCord and Sotin (2005) derived from pre-Dawn telescopic data raises the prospect of geological processes similar to those on lineated valley fills on Mars. Recent observations from Dawn data confirmed these suggestions and reveal that Ceres is partially differentiated into a rocky interior and a shell dominated by a mixture of ammoniated phyllosilicates, carbonates, salts, clathrate hydrates, and no more than 30–40% water ice (Bland et al., 2016; De Sanctis et al., 2015, 2016; Fu et al., 2017; Hiesinger et al., 2016). A dynamic isostasy model, developed by Ermakov et al. (2017), suggests that the volatile-rich outer layer have an average thickness of $41.0^{+3.2}_{-4.7}$ km.

Surface ice has been locally detected in nine locations on Ceres's surface (Combe et al., 2017). The first evidence of water ice was found in the Oxo crater, which has been exposed by mass-wasting processes (Combe et al., 2016), and regolith ice has been detected at latitudes above 40° (Prettyman et al., 2017). Measurements by the Gamma Ray and Neutron Detector suggest that ice should be present in regolith pore spaces at depths of centimeters near the poles and depths of a few meters near the equator (Prettyman et al., 2017; Schorghofer, 2016). Furthermore, Prettyman et al. (2017) propose that the dry equatorial regolith contains bound water (molecular H_2O, hydroxides, and hydroxyl groups) within a few decimeters of the surface. Features thought to be caused by water ice and/or volatile-rich material occur as domes, pits and lobate flows on Ceres's surface (Buczkowski et al., 2016; Krohn et al., 2016; Ruesch et al., 2016; Schmidt et al., 2017; Sizemore et al., 2017). The presence of pitted crater materials on Ceres at low and middle latitudes indicates the occurrence of ice in the Cerean upper regolith (Schorghofer, 2016; Sizemore et al., 2017).

Occator is a 90-km wide complex crater (Hiesinger et al., 2016). Although there is no evidence of water ice exposed on the surface within or around the Occator crater, the minerals detected on the surface are the result of aqueous activity (Ammannito et al., 2016; Combe et al., 2017; De Sanctis et al., 2015; Prettyman et al., 2017; Raponi et al., 2018). The involvement of water ice is suggested by several surface features, observed at high-resolution FC images within Occator (Krohn et al., 2016; Ruesch et al., 2018). Its interior exhibits extended plains of ponded material and extensive lobate materials, which are supposed to be formed by impact melt or cryovolcanic flows (e.g., Jaumann et al., 2017, Krohn et al., 2016, Schenk et al., 2016, Scully et al., 2018). Occator is thought to be impacted into a brine-rich crustal reservoir, triggering the mobility of material and forming extended plains as well as lobate flow features, interpreted as cryovolcanic features (Krohn et al., 2016). It is also possible that the tectonic structure at the southern part of Occator is the result of a subsurface reservoir, which is enriched in salt-bearing components driven upward by density/temperature inhomogeneity. There, a pattern of cracks indicates breaking of the plains material by upwelling, and the partly polygonal arrangements suggest formation by dehydration (Krohn et al., 2016). Furthermore, the most prominent features within Occator are some bright spots, called faculae. The faculae are thought to be formed by a liquid brine extrusion, reaching the surface at high velocity, as in a salt-water fountain (Ruesch et al., 2018).

In this paper, we analyze and discuss the likely formation processes for the ring-mold craters within Occator.

2. Methods

For our analysis of ring-mold craters, we used the Dawn FC data (Sierks et al., 2011) from the Low Altitude Mapping Orbit (LAMO) with a spatial resolution of 35 m/pixel. Furthermore, we made use of a digital terrain model stereo-photogrammetrically derived from FC Low Altitude Mapping Orbit data with a spatial resolution of 32 m/pixel (Preusker et al., 2016). The crater diameters were measured from edge to edge of the outermost recognizable circular moat. Diameter measurements for the ring-mold craters are only approximate, as their rim is not as sharp as for simple craters. The measurements are affected by impacting into an icy substrate. Due to the low resolution of the digital terrain model and the small size of the craters, their exact depth cannot be measured. To give approximate values, we used the depth-to-diameter (d/D) ratios, where d is the crater depth and D is the diameter of the crater, for the average Ceres crater, as derived by Hiesinger et al. (2016). They estimate a depth/diameter relationship for craters on Ceres of about $d = \sim 0.25D$.

3. Ring-Mold Craters on Ceres

We found 36 ring-mold craters on the crater floor of Occator with an almost circular shape, not dissimilar to simple craters. The craters seem to be subsiding into the surface, and therefore, the rims are less elevated

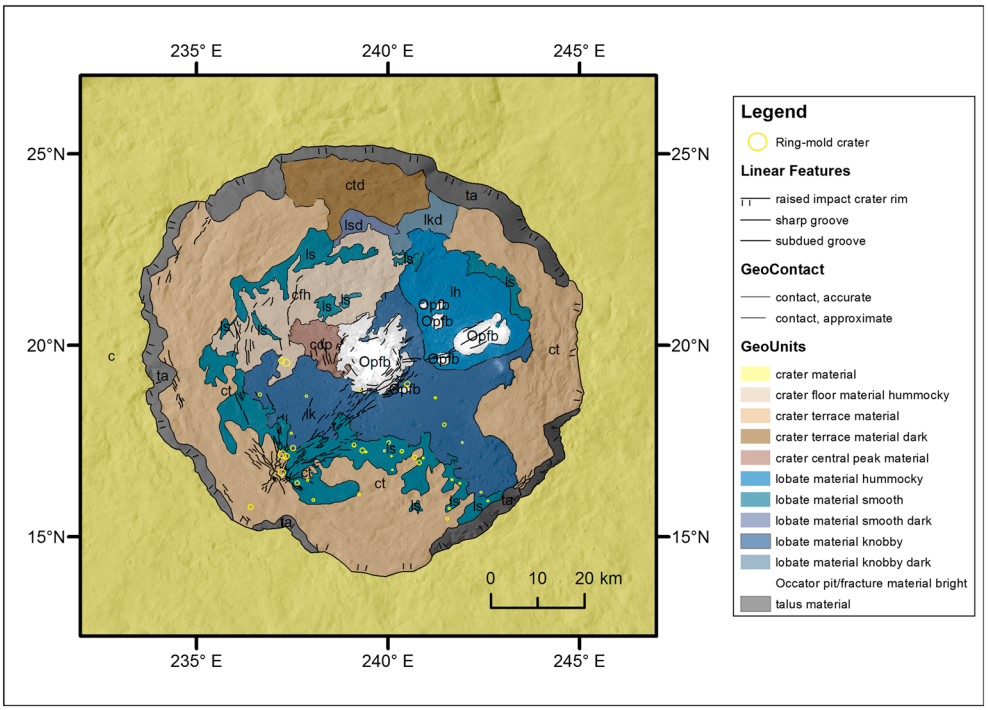

Figure 1. Simplified geological map of the Occator crater (modified after Buczkowski et al. (2017); Kargel (1991). The map shows the distribution of ring-mold craters (yellow circles) preferentially on the smooth and knobby lobate materials of the lower crater floor.

above the surrounding terrain. Their exact depth, however, is not detected in the current digital terrain model. They are concentrated on the southern crater floor. Most ring-mold craters are located on the lobate smooth material, and few craters are found on the crater terrace material (see geologic maps of Buczkowski et al., 2017, and Kargel, 1991).

Ring-mold crater diameters vary from ~280 to ~1,520 m with a mean of ~710 m. Bowl-shaped craters in this area, however, are typically smaller than ring-mold craters, with a mean of ~366 m. Larger simple craters have not formed in the geologically recent unit investigated here.

Most bowl-shaped craters are found on the higher elevated crater terraced material, interpreted as collapsed crater wall material. Only a few tiny bowl-shaped craters are found on the smooth and knobby lobate materials of the lower crater floor, whereas the majority of ring-mold craters are located on these materials (Figures 1 and 2). Several ring-mold craters are degraded and deformed by cracks or lobate material (Figures 3e–3f). Due to the spatial resolution of the Dawn FC data, we can only clearly identify ring-mold craters down to ~280 m.

Following the classification for ring-mold craters of Kress and Head (2008), we found three classes within the Occator crater: (1) central pit or bowl craters (Figure 3a); (2) central mound craters (Figure 3b); and (3) a central plateau crater (Figure 3c). The morphology of Cerean ring-mold craters is remarkably similar to ring-mold craters identified on Mars by, for example, Kress and Head (2008), Baker et al. (2010), and Pedersen and Head (2010; Figure 4).

At Ceres and Mars, ring-mold craters are generally larger than bowl-shaped craters formed by the same impactor. However, the Martian ring-mold craters with maximum diameters between 697 (mean 225 m; Baker et al., 2010) and 750 m (mean 102 m; Kress & Head, 2008) are smaller than the ring-mold craters on Ceres (max. 1,520 m).

On both planetary bodies, the ring-mold craters are nearly rimless with a circular outer moat and show a variety of interior morphologies, such as central pits or bowls, plateaus, and mounds (Figure 4). Furthermore, on Ceres and Mars, the ring-mold craters are associated with flow features. On Mars, the

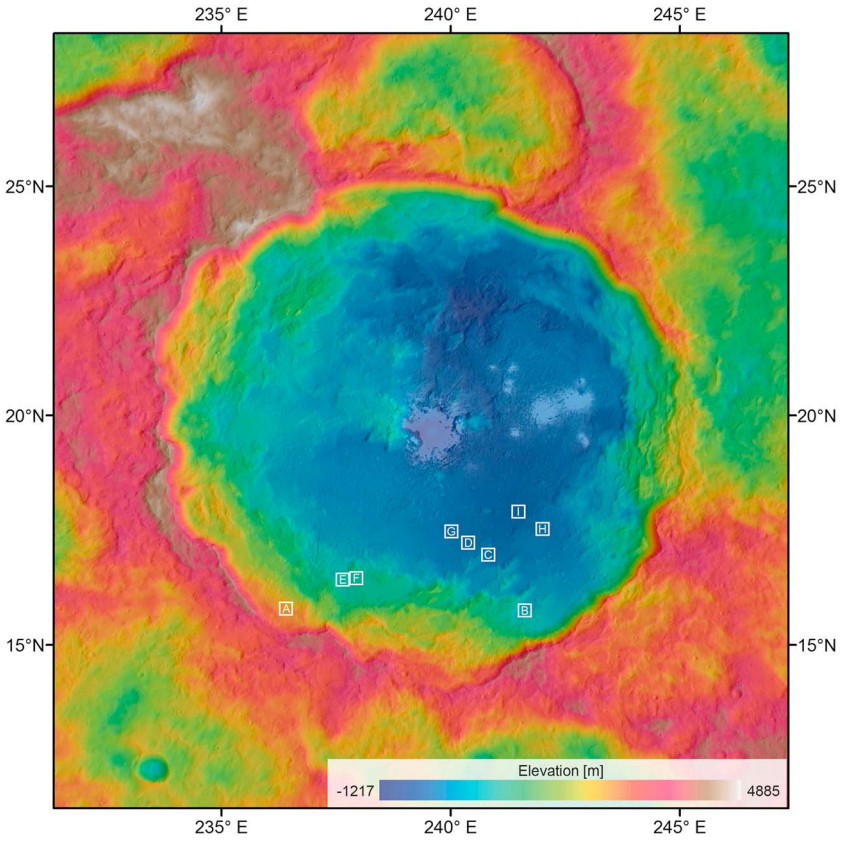

Figure 2. Topographic map of the Occator crater, showing the locations of selected ring-mold craters shown in Figure 3.

ring-mold craters occur on lineated valley fills and lobate debris aprons as well as crater-filling depressions, in which ice substrate accumulates, exhibiting concentric rings, whereas on Ceres, the ring-mold craters occur solely on lobate materials within Occator.

In general, these lobate materials show localized or pervasive evidence of flows, for example, lobate margins, streamlining, and/or ponding in topographic lows. Ring-mold craters on both planetary bodies seem to subside into the surface (Figure 4). The numerous parallels in morphology and setting between Cerean and Martian ring-mold craters suggest that the features on both bodies are analogous and likely share a common formation process.

4. Discussion

On Mars, Kress and Head (2008) attributed the distinct morphology of ring-mold craters to the presence of buried, relatively pure ice at the time of formation of the superposed crater. Impacts into a dry regolith or ice-cemented regolith look like those formed in solid rocks (basalt) and would not produce such ring-mold crater morphology (Croft et al., 1979; Kress & Head, 2008). Furthermore, experimental results by, for example, Croft et al. (1979), Kato et al. (1995), and Kawakami et al. (1983) show that impacting into nearly pure ice causes not only the unusual morphologies but also the crater diameters to be at least two times larger than for craters in basalt or regolith. This compositional effect is caused by the difference in strength of the material during the excavation phase (Holsapple & Choe, 1991; Melosh, 1989). Because of the sublimation of freshly exposed ice, raised crater rims and ejecta disappear and the shape of the resulting crater is softened (Kato et al., 1995). In addition, the modification of ring-mold craters can be affected by viscous flows in sloped terrain or by post-impact degradation processes, like sublimation of the ice-rich surface material (Baker et al., 2010). The difference in the interior morphology of ring-mold craters is interpreted as an interaction of shock impedance and strength mismatches between the surface and ice layers (Kress & Head, 2008; Quaide et al., 1965; Senft & Stewart, 2008). Deflation and sublimation of the ice-rich deposits lead to the increase of the

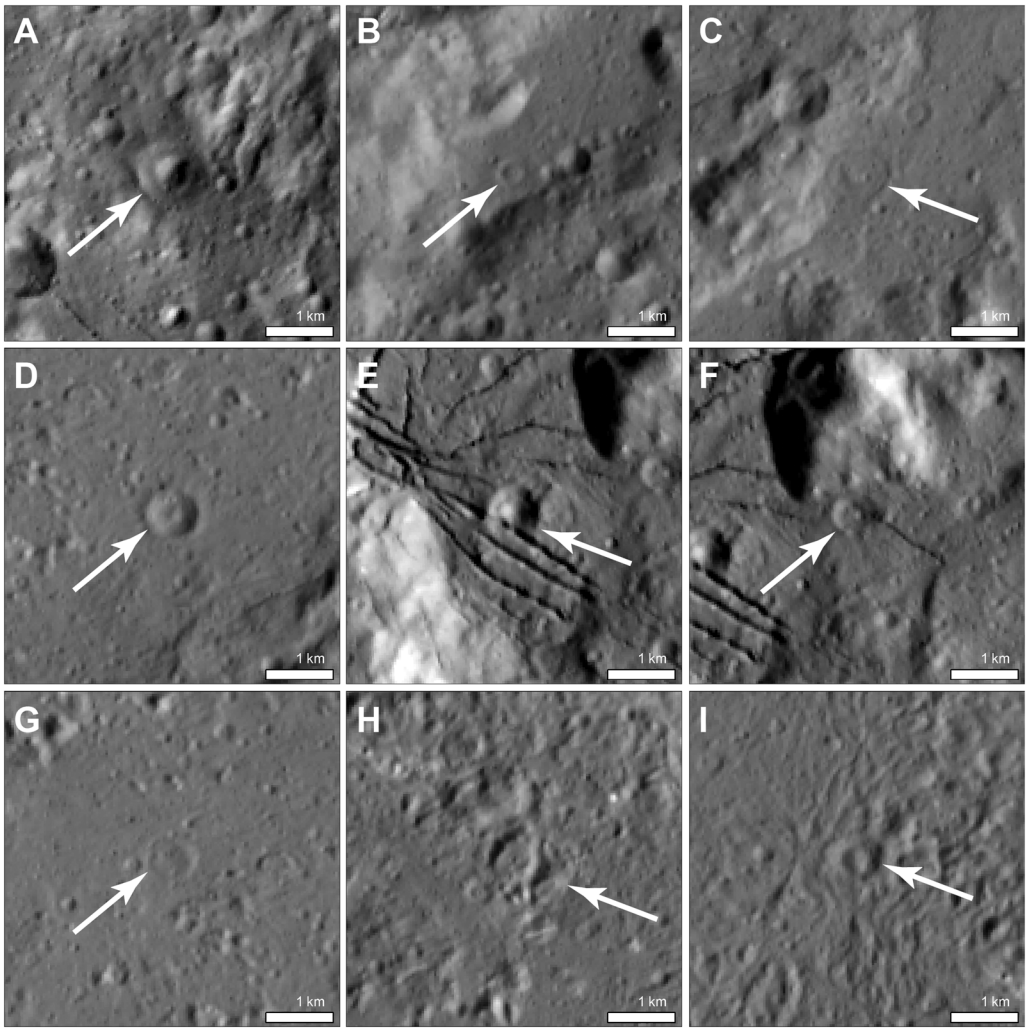

Figure 3. Examples of ring-mold craters on Ceres; white arrows point to the particular crater rims. (a) central pit/bowl (Framing Camera (FC) image FC21A0074999_16191122052F1B); (b) central mound (FC image FC21A0056967_16047193628F1C); (c) central plateau (FC image FC21A0056967_16047193628F1C); (d) central peak (FC image FC21A0056967_16047193628F1C); (e–i) ring-mold craters degraded and deformed by cracks (e and f; FC image FC21A0074999_16191122052F1B), lobate material (g; FC image FC21A0056967_16047193628F1C), and flow features (h–i; FC image FC21A0056967_16047193628F1C).

outer moat, leaving a circular plateau in the center of the crater. Further degradation of the plateau would produce a concentric pattern resulting in multiringed plateaus (Pedersen & Head, 2010). We also prefer an impact into ice formation for such craters in Occator on the basis of the following considerations.

The interior of Occator exhibits extended plains of ponded material and extensive lobate materials (Figure 2), which are supposed to be formed by impact melt or cryovolcanic flows (e.g., Jaumann et al., 2017, Krohn et al., 2016, Schenk et al., 2016). Occator is thought to be formed in a layer of hydrated salts, triggering the mobility of ice-rich material and forming such plains and flow features (Krohn et al., 2016). The crater floor of Occator has relatively larger grain size, an observation interpreted as due to slower cooling conditions in which larger grains can grow, such as, for example, in a melt reservoir (Raponi et al., 2018). Some ring-mold craters are located on or near the tectonic structure in the southern part of the Occator floor.

There, a pattern of cracks indicates breaking of the plains material and is supposed to be the result of upward-moving cryomagma. This upwelling is associated with an uplift of the Occator floor, resulting in a localized doming event (Kargel, 1995; Krohn et al., 2016). The occurrence of subsurface brines within Occator has been proposed by De Sanctis et al. (2016) on the basis of the mineralogy of the bright faculae

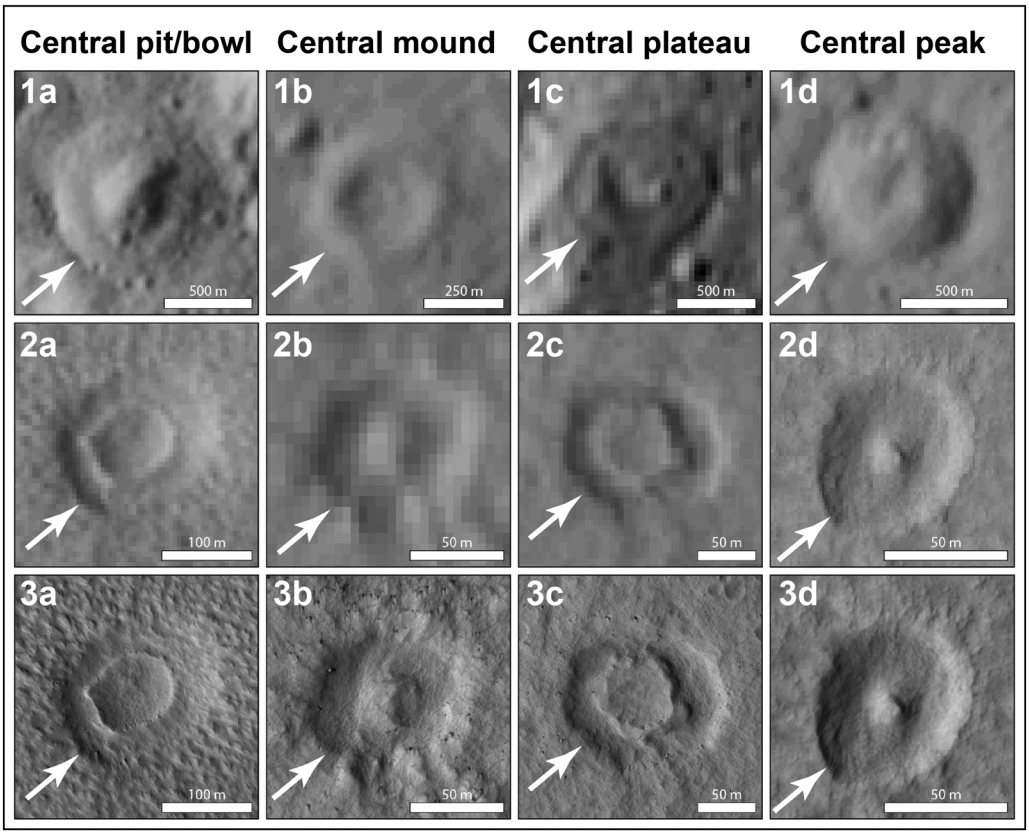

Figure 4. Comparison of different types of ring-mold craters on Ceres and Mars; white arrows point to the particular crater rims. (1a–d) The four types of ring-mold craters found on Ceres, recognized on Dawn Framing Camera image data with a mean ground resolution of 35 m/pixel. Illumination is from the right. Close-up of the craters is shown in the same order in Figure 3a–d. (2a–d) Examples of the particular types of ring-mold craters on Mars as they would appear in Context Camera data (CTX; Malin et al., 2007) resampled to the same diameter/pixel ratio of the above Ceres analogues. (3a–d) The same ring-mold craters depicted in the second row, but as they appear on High Resolution Imaging Science Experiment data (HiRISE; McEwen et al., 2007) with a resolution between 0.25 and 0.5 m/pixel. Illumination in CTX and HiRISE images is from the left. Ring-mold craters are classified as follows: Central pit/bowl: (1a) Ceres located at 236.40°E, 15.78°N; (2a) CTX image B01_009882_2204 and (3a) HiRISE image PSP_010805_2205; Mars located at 81.42°W, 40.27°N; Central mound: (2a) Ceres located at 241.59°E, 15.74°N; (2b) CTX image D02_027855_2192 and (3b) HiRISE image ESP_027855_2195; Mars located at 83.59°W, 39.06°N; Central plateau: Ceres located at 240.80°E, 16.95°N; (2c) CTX image D02_027855_2192 and (3c) HiRISE image ESP_027855_2195; Mars located at 83.58°W, 39.03°N; Central peak: (1d) Ceres located at 240.36°E, 17.23°N; (2d) CTX image ESP_017148_2205 and (3d) HiRISE image ESP_017148_2205; Mars located at 90.31°W, 40.18°N.

material. The brine consists of liquid water, carbonates, gases, and altered solids (De Sanctis et al., 2016; Zolotov, 2017). Furthermore, the bright material of the faculae within Occator is thought to be formed by a liquid brine, reaching the surface at high velocity, as in a salt-water fountain (Ruesch et al., 2018).

Therefore, it is likely that the subsurface ice at Occator is at a relatively shallow depth, below a thin protective layer of regolith, and those impacts hitting the subsurface ice layer form ring-mold craters. Additionally, the sizes of the bowl-shaped craters can be used to estimate a minimum regolith thickness. The mean bowl-shaped crater diameter in our study is ~366 m. Using the depth to diameter ratio from Hiesinger et al. (2016), we estimate that the overlying area is only several tens of meters thick. This indicates that the small bowl-shaped crater adjacent to the ring-mold craters do not penetrate to the ice layer. Furthermore, this is consistent with the findings of Ermakov et al. (2017), indicating that the volatile-rich outer layer have an average thickness of $41.0^{+3.2}_{-4.7}$ km. However, the relatively low percentage of ring-mold crater morphologies and the distribution within Occator suggest that differences in ice preservation and ice depth and content may occur within the crater. The different preservation of ice below the thin layer may be related to the inhomogeneous distribution of crater floor material. The northern part of the crater floor has a higher elevation than the southern crater floor and appears to contain layers of material (Figure 2). A massive layer of

crater terrace material, which is thought to be formed by mass wasting and collapsing crater walls shortly after the craters' formation (Scully et al., 2017), and a series of superimposing flows and spreading out from the central white spot, Cerealia Facula (Krohn et al., 2016), are distributed over the whole northern crater floor. The flows are ~200 m higher than the surrounding materials (Kargel, 1991, 1995). The southern part of Occator is lower than the northern part and consists predominantly of, besides crater terrace material, an apparently thin layer of knobby lobate and lobate materials. Thus, the differences in material thickness might explain the occurrence of ring-mold craters only in the southern part. The projectiles of ring-mold craters could be too small to penetrate through the thicker layers of the northern crater floor. It is also possible that, for example, within the range of the faculae, ring-mold craters have been covered by the fresher material excavated from the faculae or other flow material.

5. Conclusion

We find that the water ice within Occator was shallow enough to modify impact craters and produce ring-mold crater morphologies. The occurrence of bowl-shaped craters with relatively small crater diameters adjacent to ring-mold craters with larger diameters implies that either the bowl-shaped craters did not penetrate through the debris layer to the ice-rich layer below or the ice is distributed inhomogeneously, for example, in subsurface lenses. The observation of ring-mold craters can be used to detect regolith-covered ice layers and to estimate the depth to the ice and thickness of overlying till by calculating the maximum depth of the associated bowl-shaped craters (Baker et al., 2010; Kress & Head, 2008). The most recent thickness may be estimated by the largest and most pristine bowl-shaped craters, whereas the initial diameter of ring-mold craters can be used to detect the boundary between ice and overlying debris-rich layers (Kress & Head, 2009). Moreover, the occurrence of ring-mold craters on the surface is a sign for localized water ice reservoirs in the subsurface and can be used for the study of habitable zones on planetary bodies.

Acknowledgments
We thank the Dawn team for the development, cruise, orbital insertion, and operations of the Dawn spacecraft at Ceres. Portions of this work were performed at the DLR Institute of Planetary Research, at the Jet Propulsion Laboratory (JPL) under contract with NASA, as well as the German Aerospace Center (DLR). Dawn data are archived with the NASA Planetary Data System https://sbn.psi.edu/pds/resource/dawn/dwncfcL1.html. K. Krohn is supported by the Helmholtz Association (HGF) through the research Helmholtz Postdoc Program. We acknowledge the careful and highly beneficial review by an anonymous referee.

References

Ammannito, E., DeSanctis, M. C., Ciarniello, M., Frigeri, A., Carrozzo, F. G., Combe, J.-P., et al. (2016). Distribution of phyllosilicates on the surface of Ceres. *Science*, *353*, aaf4279. https://doi.org/10.1126/science.aaf4279

Baker, D. M. H., Head, J. W., & Marchant, D. R. (2010). Flow patterns of lobate debris aprons and lineated valley fill north of Ismeniae Fossae, Mars: Evidence for extensive mid-latitude glaciation in the Late Amazonian. *Icarus*, *207*(1), 186–209. https://doi.org/10.1016/j.icarus.2009.11.017

Bland, M. T., Raymond, C. A., Schenk, P. M., Fu, R. R., Kneissl, T., Pasckert, J. H., et al. (2016). Composition and structure of the shallow subsurface of Ceres revealed by crater morphology. *Nature Geoscience*, *9*(7), 538–542. https://doi.org/10.1038/ngeo2743

Buczkowski, D. L., Schmidt, B. E., Williams, D. A., Mest, S. C., Scully, J. E. C., Ermakov, A. I., et al. (2016). The geomorphology of Ceres. *Science*, *353*, aaf4332. https://doi.org.10.1126/science.aaf4332

Buczkowski, D. L., Williams, D. A., Scully, J. E. C., Mest, S. C., Crown, D. A., Schenk, P. M., et al. (2017). The geology of the occator quadrangle of dwarf planet Ceres: Floor-fractured craters and other geomorphic evidence of cryomagmatism. *Icarus*, 1–12. https://doi.org/10.1016/j.icarus.2017.05.025

Combe, J.-P., McCord, T. B., Tosi, F., Ammannito, E., Carrozzo, F. G., De Sanctis, M. C., et al. (2016). Detection of local H_2O exposed at the surface of Ceres. *Science*, *353*, aaf3010. https://doi.org/10.1126/science.aaf3010

Combe, J.-P., Raponi, A., Tosi, F., de Sanctis, M. C., Carrozzo, F. G., Zambon, F., et al. (2017). Exposed H_2O-rich areas detected on Ceres with the dawn visible and infrared mapping spectrometer. *Icarus*, 1–20. https://doi.org/10.1016/j.icarus.2017.12.008

Croft, S. K., Kieffer, S. W., & Ahrens, T. J. (1979). Low-velocity impact craters in ice and ice-saturated sand with implications for Martian crater count ages. *Journal of Geophysical Research*, *84*(B14), 8023–8032. https://doi.org/10.1029/JB084iB14p08023

De Sanctis, M. C., Ammannito, E., & Russell, C. T. (2015). Ammoniated phyllosilicates with a likely outer Solar System origin on (1) Ceres. *Nature*, *528*(7581), 241–244. https://doi.org/10.1038/nature16172

De Sanctis, M. C., Raponi, A., & Russell, C. T. (2016). Bright carbonate deposits as evidence of aqueous alteration on (1) Ceres. *Nature*, *536*(7614), 54–57. https://doi.org/10.1038/nature18290

Ermakov, A. I., Fu, R. R., Castillo-Rogez, J. C., Raymond, C. A., Park, R. S., Preusker, F., et al. (2017). Constraints on Ceres' internal structure and evolution from its shape and gravity measured by the Dawn spacecraft. *Journal of Geophysical Research: Planets*, *122*, 2267–2293. https://doi.org/10.1002/2017JE005302

Fu, R. R., Ermakov, A. I., Marchi, S., Castillo-Rogez, J. C., Raymond, C. A., Hager, B. H., et al. (2017). The interior structure of Ceres as revealed by surface topography. *Earth and Planetary Science Letters*, *476*, 153–164. https://doi.org/10.1016/j.epsl.2017.07.053

Hiesinger, H., Marchi, S., Schmedemann, N., Schenk, P., Pasckert, J. H., Neesemann, A., et al. (2016). Cratering on Ceres: Implications for its crust and evolution. *Science*, *353*, aaf4759. https://doi.org/10.1126/science.aaf4759

Holsapple, K. A., & Choe, K. Y. (1991). Energy coupling in catastrophic collisions. NASA, Washington, Reports of Planetary Geology and Geophysics Program (pp 352–353).

Jaumann, R., Preusker, F., Krohn, K., von der Gathen, I., Stephan, K., Matz, K.-D., et al. (2017). Topography and geomorphology of the interior of Occator crater on Ceres. *Lunar and Planetary Science Conference*, *48*, 1440.

Kargel, J. S. (1991). Brine volcanism and the interior structures of asteroids and icy satellites. *Icarus*, *94*(2), 368–390. https://doi.org/10.1016/0019-1035(91)90235-L

Kargel, J. S. (1995). Cryovolcanism on the icy satellites. *Earth, Moon, and Planets*, *67*, 101–113.

Kato, M., Iijima, Y.-I., Arakawa, M., Okimura, Y., Fujimura, A., Maeno, N., et al. (1995). Ice-on-ice impact experiments. *Icarus*, *113*(2), 423–441. https://doi.org/10.1006/icar.1995.1032

Kawakami, S., Mizutani, H., Takagi, Y., Kato, M., & Kumazawa, M. (1983). Impact experiments on ice. *Journal of Geophysical Research*, *88*(B7), 5806–5814. https://doi.org/10.1029/JB088iB07p05806

Kress, A. M., & Head, J. W. (2008). Ring-mold craters in lineated valley fill and lobate debris aprons on Mars: Evidence for subsurface glacial ice. *Geophysical Research Letters*, *35*, L23206. https://doi.org/10.1029/2008GL035501

Kress, A. M., & Head, J. W. (2009). Ring-mold craters on lineated valley fill, lobate debris aprons, and concentric crater fill on Mars: Implications for near-surface structure, composition, and age. *Lunar and Planetary Science Conference*, *40*, 1379.

Krohn, K., Jauman, R., Stephan, K., Otto, K. A., Schmedemann, N., Wagner, R. J., et al. (2016). Cryogenic flow features on Ceres: Implications for crater-related cryovolcanism. *Geophysical Research Letters*, *43*, 1–10. https://doi.org/10.1002/2016GL070370

Malin, M. C., Bell, J. F. III, Cantor, B. A., Caplinger, M. A., Calvin, W. M., Todd Clancy, R., et al. (2007). Context Camera Investigation on board the Mars reconnaissance orbiter. *Journal of Geophysical Research*, *112*, E05S04. https://doi.org/10.1029/2006JE002808

Mangold, N. (2003). Geomorphic analysis of lobate debris aprons on Mars at Mars orbiter camera scale: Evidence for ice sublimation initiated by fractures. *Journal of Geophysical Research*, *108*(E4), 8021. https://doi.org/10.1029/2002JE001885

McCord, T. B., & Sotin, C. (2005). Ceres: Evolution and current state. *Journal of Geophysical Research*, *110*, E05009. https://doi.org/10.1029/2004JE002244

McEwen, A. S., Eliason, E. M., Bergstrom, J. W., Bridges, N. T., Hansen, C. J., Alan Delamere, W., et al. (2007). Mars reconnaissance Orbiter's high resolution imaging science experiment (HiRISE). *Journal of Geophysical Research*, *112*, E05S02. https://doi.org/10.1029/2005JE002605

Melosh, H. J. (1989). *Impact cratering: A geologic process*. New York: Oxford University Press.

Pedersen, G. B. M., & Head, J. W. (2010). Evidence of widespread degraded Amazonian-aged ice-rich deposits in the transition between Elysium Rise and Utopia Planitia, Mars: Guidelines for the recognition of degraded ice-rich materials. *Planetary and Space Science*, *58*(14-15), 1953–1970. https://doi.org/10.1016/j.pss.2010.09.019

Prettyman, T. H., Yamashita, N., Toplis, M. J., McSween, H. Y., Schörghofer, N., Marchi, S., et al. (2017). Extensive water ice within Ceres' aqueously altered regolith: Evidence from nuclear spectroscopy. *Science*, *355*(6320), 55–59. https://doi.org/10.1126/science.aah6765

Preusker, F., Scholten, F., Matz, K.-D., Elgner, S., Jaumann, R., Roatsch, T., et al. (2016). Dawn at Ceres — Shape model and rotational state. *Lunar and Planetary Science Conference*, *47*, 1954.

Quaide, W. L., Gault, D. E., & Schmidt, R. A. (1965). Gravitative effects on lunar impact structures. *Annals of the New York Academy of Sciences*, *123*(2), 563–572. https://doi.org/10.1111/j.1749-6632.1965.tb20388.x

Raponi, A., de Sanctis, M. C., Carrozzo, F. G., Ciarniello, M., Castillo-Rogez, J. C., Ammannito, E., et al. (2018). Mineralogy of Occator crater on Ceres and insight into its evolution from the properties of carbonates, phyllosilicates, and chlorides. *Icarus*, 1–14. https://doi.org/10.1016/j.icarus.2018.02.001

Ruesch, O., Platz, T., Schenk, P., McFadden, L. A., Castillo-Rogez, J. C., Quick, L. C., et al. (2016). Cryovolcanism on Ceres. *Science*, *353*, aaf4286.

Ruesch, O., Quick, L. C., Landis, M. E., Sori, M. M., Čadek, O., Brož, P., et al. (2018). Bright carbonate surfaces on Ceres as remnants of salt-rich water fountains. *Icarus*, 1–10. https://doi.org/10.1016/j.icarus.2018.01.022

Schenk, P., Marchi, S., O'Brien, D. P., Bland, M., Platz, T., Hoogenboom, T., et al. (2016). Impact cratering on the small planets Ceres and Vesta: S-C transitions, central pits, and the origin of bright spots. *Lunar and Planetary Science Conference*, *47*, 2697.

Schmidt, B. E., Hughson, K. H. G., Chilton, H. T., Scully, J. E. C., Platz, T., Nathues, A., et al. (2017). Geomorphological evidence for ground ice on dwarf planet Ceres. *Nature Geoscience*, *10*(5), 338–343. https://doi.org/10.1038/ngeo2936

Schorghofer, N. (2016). Predictions of depth-to-ice on asteroids based on an asynchronous model of temperature, impact stirring, and ice loss. *Icarus*, *276*, 88–95. https://doi.org/10.1016/j.icarus.2016.04.037

Scully, J. E. C., Buczkowski, D. L., Neesemann, A., Williams, D. A., Mest, S. C., Raymond, C. A., et al. (2017). Ceres' Ezinu quadrangle: A heavily cratered region with evidence for localized subsurface water ice and the context of Occator crater. *Icarus*, 1–17. https://doi.org/10.1016/j.icarus.2017.10.038

Scully, J. E. C., Buczkowski, D. L., Raymond, C. A., Bowling, T., Williams, D. A., Neesemann, A., et al. (2018). Ceres' Occator crater and its faculae explored through geologic mapping. *Icarus*, 1–18. https://doi.org/10.1016/j.icarus.2018.04.014

Senft, L. E., & Stewart, S. T. (2008). Impact crater formation in icy layered terrains on Mars. *Meteoritics and Planetary Science*, *43*(12), 1993–2013. https://doi.org/10.1111/j.1945-5100.2008.tb00657.x

Sierks, H., Keller, H. U., Jaumann, R., Michalik, H., Behnke, T., Bubenhagen, F., et al. (2011). The Dawn framing camera. *Space Science Reviews*, *163*(1-4), 263–327. https://doi.org/10.1007/s11214-011-9745-4

Sizemore, H. G., Platz, T., Schorghofer, N., Prettyman, T. H., de Sanctis, M. C., Crown, D. A., et al. (2017). Pitted terrains on (1) Ceres and implications for shallow subsurface volatile distribution. *Geophysical Research Letters*, *44*, 6570–6578. https://doi.org/10.1002/2017GL073970

Zolotov, M. Y. (2017). Aqueous origins of bright salt deposits on Ceres. *Icarus*, *296*, 289–304. https://doi.org/10.1016/j.icarus.2017.06.018